Eur Biophys J (1994) 22:399–403

European Biophysics Journal

The voltage-dependent H^+-ATPase of the sugar beet vacuole is reversible

Franco Gambale [1], H. Albert Kolb [2], Alberto M. Cantù [1], Rainer Hedrich [3]

[1] Istituto di Cibernetica e Biofisica, Via Dodecaneso 33, I-16146 Genova, Italy
[2] Institut für Physiologie, Universität Tübingen, Gmelinstrasse 5, D-72076 Tübingen, Germany
[3] Institut für Biophysik, Universität Hannover, Herrenhäuserstrasse 2, D-30419 Hannover, Germany

Received: 1 April 1993 / Accepted in revised form: 14 October 1993

Abstract. The vacuolar H^+-ATPase is essential for the creation and maintenance of solute gradients. Knowledge of the reversal potential, expressed by the voltage and pH dependence of the pump may allow to determine the activity range of the enzyme. In the whole-vacuole configuration of the patch-clamp technique the application of Mg-ATP elicited inward-directed currents through the H^+-ATPase. Reversal of the pump current was obtained in the presence of a pH gradient across the membrane (inside acid) by replacement of Mg-ATP by Mg-ADP and P_i. The active nature of this nucleotide-dependent transport process is reflected by a Q_{10} of 3.2. The voltage-dependence of the pump was elucidated by voltage-steps to various depolarizing and hyperpolarizing potentials. In the presence of Mg-ATP the current-voltage relationship of the pump current is characterized by an almost linear increase of the steady state current between 20 mV and 100 mV, tending to saturate at more positive potentials. The voltage-dependence of the inward pump current could be described by a pseudo-two-state model.

Key words: Electrogenic pumps – Vacuolar-type – Voltage-dependence – Temperature-dependence – Reversion

Introduction

Vacuolar type (V-type) H^+-ATPases represent an ubiquitous group of proton pumps that are found in organelles such as vacuoles of plants and fungi, as well as lysosomes, endosomes, secretory and storage granules (Schneider 1987; Hedrich et al. 1989; Forgac 1989; Läuger 1991). Proton pumps are responsible for the energization of the vacuolar membrane and acidification of the enclosed intracellular compartments.

Correspondence to: R. Hedrich

Previous patch-clamp studies on isolated sugar beet vacuoles have demonstrated that H^+ pumps can be activated by "cytoplasmic" Mg-ATP (Hedrich et al. 1986). Application of Mg-PP_i in addition to Mg-ATP unequivocally demonstrated that two H^+-pumps, a H^+-ATPase and a H^+-PP_i ase are located in the same membrane (Hedrich and Kurkdjian 1988; Hedrich et al. 1989).

Difficulties in studying the electrical properties of ionic pumps derive from the fact that whole-cell pump currents are small and easily masked by ion-channel currents, especially by SV-type channel currents through the vacuolar membrane (Hedrich et al. 1986; Hedrich and Neher 1987; Lohse and Hedrich 1992) analyzed in this study. The resolution limit is a consequence of the fact that the amount of charge moved per unit time by a single active transporter, pump or carrier molecule, is expected to be at least three orders of magnitude smaller than currents through an open ion channel. Thus, signals caused by the activation of single pump molecules are well beyond the resolution of the current-voltage amplifiers presently available. Instead, the whole-cell configuration, allowing the concerted activation of all pump molecules in the entire membrane surface, enabled us to analyze H^+ currents through the vacuolar ATPase and to characterize the voltage-dependence of this electroenzyme in the physiological voltage range. Under conditions which largely supressed ion channel activity, we studied the temperature- and voltage-dependence and direction of the steady-state H^+-current generated by the V-type ATPase.

Material and methods

Vacuole isolation

Sugar beet vacuoles were obtained from fresh taproots as described before (Coyaud et al. 1987). Cutting a thin slice of tissue and rinsing the surface with a few drops of bathing solution allowed vacuoles to be extruded directly into the recording chamber. The osmolarity of the taproot was measured and the osmotic pressure of the solutions adjusted accordingly by addition of D-sorbitol.

Seal formation and whole-vacuole recordings

Patch-clamp measurements were performed on isolated sugarbeet vacuoles using the whole-vacuole configuration. Access to the vacuole interior was gained by breaking the membrane under the patch pipette by 1 ms voltage pulses of $\pm 0.6-1.0$ V. The ionic current was recorded with a List EPC7 current-voltage amplifier and stored on a video cassette recorder equipped with a PCM Sony F1, modified according to Bezanilla (1985). Data were digitized using an Instrutech A/D/A board (Instrutech, Elmont, N.Y.) interfaced to a personal computer Atari 4Mega ST. The series of step voltages were generated by a personal computer. Current responses were simultaneously stored on hard disk. Analysis was done off line both on the Atari personal computer and on a 386 MS-DOS compatible system.

Perfusion pipettes

The bathing medium of the vacuole could be changed in a few seconds by a 'fast' perfusion system (second range) from standard bath solution (control) to bath + ATP (or ADP + P_i) and vice versa. The volume flow and the position of the pipettes was optimized with respect to the speed of solute exchange and maintenance of whole-vacuole configuration. Briefly two perfusion pipettes with a tip diameter of about ten micrometers were filled with solution and mounted on a holder connected to a hydraulic manipulator. The position of the pipettes could be manually adjusted and thereby vacuoles could be rapidly exposed to the different solutions. In order to test the effects of ATP and ADP on the same vacuole, a system based on three perfusion pipettes (control/+ATP/+ADP, see Fig. 3a) was used. A peristaltic pump connected to reservoir containing the bath solution was continuously running throughout the experiment to prevent ATP or ADP contamination from the perfusion pipettes.

The resistance of the patch pipettes was in the 2–5 Mohm range and the seal resistance was >10 Gohm. Pump current measurements were performed on vacuoles, 20–40 μm in diameter.

Results and discussion

At cytoplasmic calcium concentrations above 1 μM ('high-calcium' media) a voltage dependent SV-type (slow vacuolar) channel is the main charge carrier of the vacuolar membrane (Hedrich and Neher 1987; see Hedrich and Schroeder 1989 for review). These predominant passive ion fluxes were recorded in the whole-vacuole configuration in the presence of symmetrical solutions of 100 mM KCl in the bath and pipette. From voltage-step current relaxation experiments the steady-state current could be derived as a function of the membrane potential (Fig. 1). In this electrolyte solution the current adopts an expected zero current reversal potential of about 0 mV (deduced from tail current experiments, cf. Hedrich et al. 1986). At negative potentials a slope conductance of about $3 \cdot 10^{-8}$ S/vacuole ($2 \cdot 10^{-3}$ S/cm^2) was obtained.

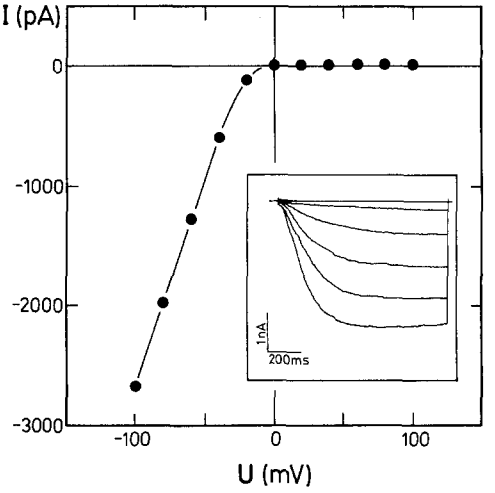

Fig. 1. Inward rectifying currents, the major ionic component of the vacuolar membrane. Steady-state current-voltage relation of SV-type channels in the whole vacuole. Inset: Slow activating voltage-dependent currents were elicited upon hyperpolarization of the membrane. The vacuole was clamped to 0 mV and stepped to various potentials between +100 and −100 mV during 1 s voltage pulses. Ionic composition of the bath and pipette solution were: KCl 100 mM, $CaCl_2$ 1 mM, $MgCl_2$ 2 mM, Hepes/KOH pH 7 and sorbitol to adjust a final osmotic pressure of 760 mOsmol

For positive voltages the current exhibits a steep inward rectification. These slow activating inward currents did not inactivate even during prolonged voltage stimulation (Fig. 1 inset). In the presence of 0.1–1 mM external calcium the membrane resistance in the physiological voltage range of the H^+-ATPase (about −20 to 100 mV, vacuolar side relative to the cytoplasm) was >1 Gohm. Therefore 'high-calcium' media were selected to study the voltage dependence of the H^+-pump. The I–U characteristics of the whole vacuole, however, indicated that ATP-dependent currents could be resolved reliably only between −20 mV +100 mV. In this voltage range pump currents could be resolved without using channel blockers (Hedrich and Kurkdjian 1988).

In order to distinguish between active (ATP-driven) and passive ion transport pathways the electrical properties of the vacuolar membrane have been determined in the absence and presence of Mg-ATP. By clamping the membrane at the zero-current potential of about 0 mV, inward currents were elicited by cytoplasmic Mg-ATP (Mg-ATP in the bath solution). The upward arrow in Fig. 2 indicates the change in position of the superfusion pipette containing only the bath solution (control) to 5 mM Mg-ATP medium (see materials and methods). The onset of inward current reflects the availability of Mg-ATP to drive the pump process. During perfusion with Mg-ATP inward H^+-currents reached peak values of about 10–150 pA/vacuole (0.5 μA/cm^2 in Fig. 2c). The corresponding difference of vacuolar currents (Fig. 2c) in the absence and presence of Mg-ATP, as derived from Fig. 2b, can be considered as the net pump current. Under current-clamp the resting potential of the vacuole shown in Fig. 2a shifted reversibly from −7 mV to +42 mV during Mg-ATP superfusion.

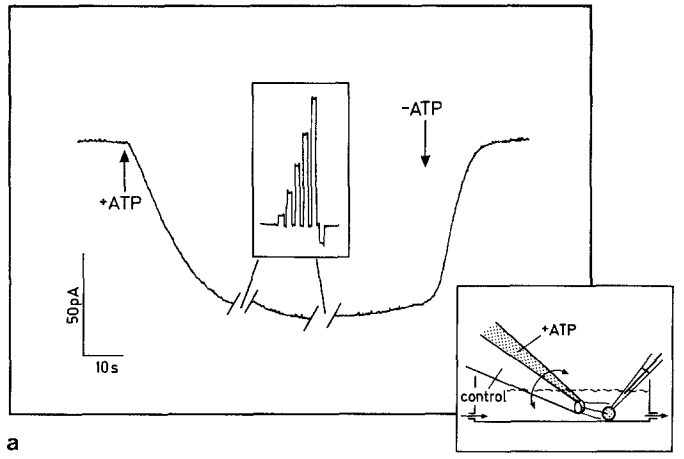

a

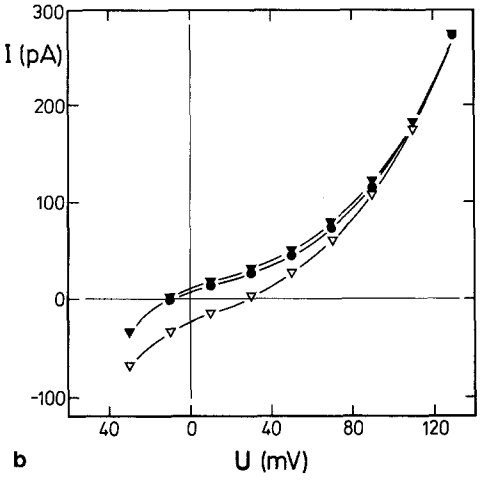

b

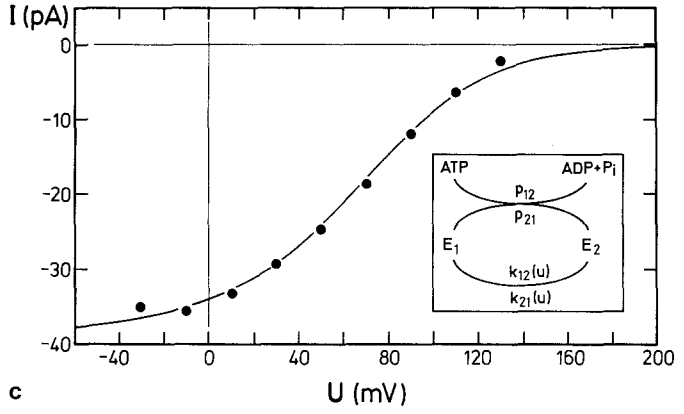

c

Fig. 2a–c. ATP-induced inward currents through the vacuolar H^+-ATPase. **a** The vacuole was clamped at a holding potential of 0 mV. Arrows indicate the times where the position of the perfusion pipette facing the vacuole was changed between control and 5 mM Mg-ATP solution. *Lower inset:* Application and withdrawal of Mg-ATP through alternating position of the two perfusion pipettes in front of the vacuole. In each experiment the two solutions were applied several times. *Upper inset:* Voltage-staircases of 20 mV increments were applied as indicated to study the voltage-dependence of the H^+-ATPase. Ionic solutions in the bath and pipette were: KCl 100 mM, $MgCl_2$ 5 mM, $CaCl_2$ 10 μM, citrate/KOH 20 mM pH 8, and sorbitol to adjust a final osmotic pressure of 990 mOsmol. **b** Steady-state whole-vacuolar currents in the absence (▲ before ATP-treatment) and ● after ATP-removal and presence (△) of 5 mM Mg-ATP as a function of membrane potential. With the vacuole clamped to a holding potential of 0 mV, voltage-staircases (see **a**) were applied after the currents had reached a steady state under the various experimental conditions applied. **c** Voltage-dependence of the vacuolar H^+-pump current obtained as difference from the data of **b**. Current-voltage relation of the electrical properties of the vacuolar membrane under ±Mg-ATP conditions represent the net pump current. The curve is fitted by Eq. (1) using the following parameters: $Nd = 10^{-7}$ mol · m^{-2}, $p_{12} = 63.5\ s^{-1}$, $p_{21} = 0\ s^{-1}$, $k_{12}(0) = 35\ s^{-1}$, $k_{21}(0) = 690\ s^{-1}$. $z = 1$ was assumed for the number of protons transported per pump cycle. *Inset:* Two-state reaction scheme of the V-type ATPase. For a theoretical description of the H^+-pump we assumed only one voltage-dependent step in the reaction cycle. In this case the steady-state current voltage relation can be described by a symbolic two-state scheme. This pseudo two-state model consists of two fictitious states E1 and E2 of the pump cycle that are connected by a voltage-dependent transition

When an H^+-gradient of four pH units was established across the membrane (pH 4 inside and pH 8 outside) and the extravacuolar face was exposed to ADP and P_i, outward currents indicate the reversal of the pump (Fig. 3a and b). The interconversion of outward current into inward current, by the change in energy charge only (Fig. 3a) indicates that both processes are related. As a consequence of H^+ release, which would result in ATP synthesis, the membrane potential shifts to more negative values (Fig. 3; current clamp).

Besides the nucleotide-dependence (Figs. 2a and 3 Hedrich et al. 1986 and 1989), the active nature of this H^+-transport system was verified by its temperature sensitivity. The temperature dependence of the vacuolar H^+-ATPase was monitored during the change in the bath temperature from 22 to 12 °C (Fig. 4). The decrease in the pump-current amplitude represents a Q_{10} value of 3.2 which corresponds to an activation energy of 87 kJ/mol for the entire transport process. For clearer presentation the vacuolar current was not plotted on an expanded time scale, but a 'knick' (Overath and Träuble 1973; Overath et al. 1975) could not be observed, indicating a change in pump activity rather than a phase transition in the lipid matrix.

The rise time of the pump current (e.g. Fig. 2a, lower inset) results from the time needed for ATP-containing solutions to replace the control solution. The time required to reach 50% of the Mg-ATP-induced steady-state current ranged between a few and 10 s, owing to variations in the position of the perfusion pipette in front of the vacuole (Fig. 2a lower inset).

Under steady-state conditions in the presence (Fig. 2a, upper inset) or absence of Mg-ATP a sequence of voltage steps (ranging from −30 mV to +130 mV) were applied from the holding potential. During the voltage pulse pump currents reached a new steady-state within 20 ms (not shown). A reliable analysis of the voltage-dependent kinetics of the ATP-induced currents were, however, hindered by the large capacitance of the vacuole (> 15 pF). In accordance with the inward current measured in the presence of Mg-ATP the currents elicited during individual voltage pulses shifted towards more negative values. The corresponding I–U characteristics measured before (filled triangles), during (open triangles) application and after removal of Mg-ATP (filled circles) are illustrated in Fig. 2b.

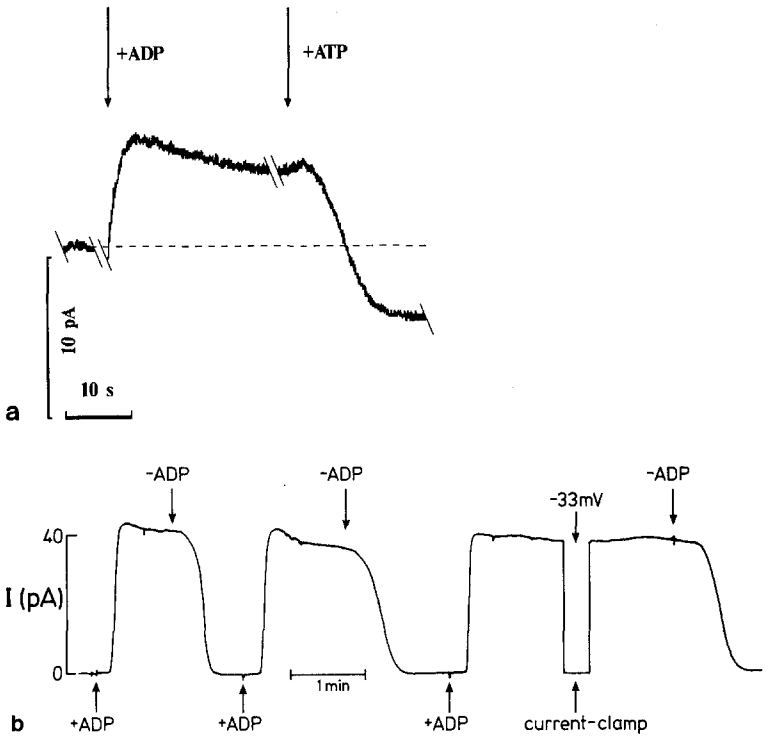

Fig. 3. **a** Inward and outward H^+ currents through the vacuolar ATPase. Inward and outward currents across the vacuolar membrane following application of "cytosolic" 5 mM Mg-ADP and its replacement by 5 mM ATP in the presence of 10 mM KP_i and a proton gradient across the vacuolar membrane ($pH_{bath}=8$ and $pH_{vacuole}=4$). **b** Reversion of the proton-pump. ADP and P_i induced outward-currents and hyperpolarization in energized (ΔpH) vacuoles. Application of "cytosolic" 5 mM Mg-ADP in the presence of 10 mM KP_i and a proton gradient across the vacuolar membrane ($pH_{bath}=8$ and $pH_{vacuole}=4$) elicited H^+-currents of about 40 pA at a holding potential of 0 mV. At the time indicated we switched from voltage-clamp to current-clamp to monitor the free-running membrane potential. Ionic solutions were: 100 mM KCl, 10 mM $MgCl_2$, 1 mM $CaCl_2$, 20 citric acid pH 4 in the pipette and 100 mM KCl, 10 mM $MgCl_2$, 1 mM K_2HPO_4, 20 citric acid pH 8 in the bath. The osmotic pressure was adjusted to 1 000 mosmol with D-sorbitol

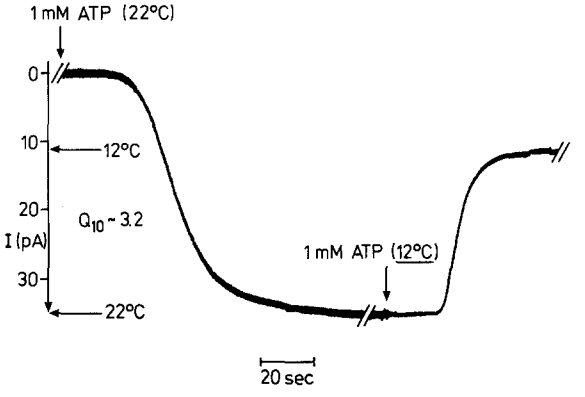

Fig. 4. Temperature-dependence of the vacuolar H^+-pump. The vacuole was clamped to 0 mV at 22 °C. The arrow indicates application of 1 mM Mg-ATP to the cytosolic face of the membrane. After ATP-induced vacuolar currents reached a steady-state the bath temperature was reduced to 12 °C. Corresponding steady-state currents measured at 22 and 12 °C are indicated on the vertical scale. For electrolyte solutions see Fig. 1

Note, that there was almost no difference between values recorded before (control) and after the Mg-ATP treatment (recovery). The voltage-dependent activity of this electroenzyme, as obtained from Fig. 2c (see above), was almost linear throughout the physiological voltage range (20 – 100 mV), tending to saturate at voltages higher than 100 mV. Analysis at more extreme voltages was difficult owing to the increase of passive currents at depolarizing potentials and to the very steep activation of SV channels at hyperpolarizing potentials (see Fig. 1).

Since activation of a proton-dependent transport system by its substrate, the proton, was not possible, we identified the H^+-pump I–U from the difference in vacuolar currents in the absence and presence of Mg-ATP (Fig. 2c). Corresponding kinetic analysis of the I–U curve was performed in terms of the minimal-reaction scheme of the proton pump, the pseudo two-state model (Hansen et al. 1981). The model consists of two states E1 (protonated) and E2 (deprotonated) within the pump cycle that are connected by a voltage-dependent transition in parallel with a voltage-independent step (Fig. 2c, inset). The steady-state current can thus be expressed as:

$$I(u)=z\cdot e_0\cdot N\cdot d\,\frac{k_{12}(u)\,p_{21}-k_{21}(u)\,p_{12}}{k_{12}(u)+k_{21}(u)+p_{12}+p_{21}}. \quad (1)$$

Assuming a symmetrical dielectric (Eyring) membrane barrier, the following relations hold:

$$k_{12}(u)=k_{12}(0)\exp(zu/2) \quad (2)$$

$$k_{21}(u)=k_{21}(0)\exp(-zu/2) \quad (3)$$

$u=FU/RT$ denotes the reduced potential, N the number of pump molecules contributing to $I(u)$, F Faraday constant, R gas constant, T absolute temperature. The prefactor d, as well as the rate constants are phenomenological fit-parameters to which an explicit meaning can be assigned only a posteriori in terms of the 'real' multi-state reaction cycle (Läuger 1991). z gives the valency of the translocated ion in a single turnover of the ATPase. The pump I–U curves measured within the voltage-range tolerated by the vacuolar membrane did not allow the application of a real multi-state model, even though additional states might exist (Läuger 1991).

Assuming an apparent z of 1, a least squares fit of Eq (1) to the experimental data of the ATP-dependent I–U curve yields a sufficient description of the transport process. It is obvious that application of Eq. (1) for a descrip-

tion of Fig. 2c allows no independent determination of the value of z since the real multi-state reaction cycle and therefore the multiplicator d is not known. The determination of the real valency z requires additional information about the number of moles of ATP hydrolyzed with respect to charge transport. The appearance of proton gradients of about 5–6 pH units between the cytoplasm and vacuole interior (e.g. lemon fruits or brown algae; for review see Hedrich and Schroeder 1989), however, provides evidence for an apparent ATP/H^+ stoichiometry of 1 rather than 2 (Sze et al. 1992).

The rate constants (see legend to Fig. 2c), indicate that the rate limiting step is the hydrolysis of ATP ($p_{12}=63.5\ s^{-1}$), while $p_{21}=0$ the reverse reaction in the cycle is negligible. These numbers are in agreement with the absence of ADP and P_i in the experiments of Fig. 2. The presence of both reaction partners at the cytoplasmic face of the H^+-pump on the other hand enables ATP synthesis (Fig. 3). Reversal of the pump around 0 mV (far from equilibrium) seems thus to be energized by the chemical gradient of the H^+ (about −230 mV; pH 8 in the cytoplasm and pH 4 inside the vacuole).

Our observations thus allow us to describe the mechanistic properties of ATP synthesis according to Senior 1988 (see also Läuger 1991), where ADP and P_i bind tightly to the electroenzyme with high affinity. In the bound form, ATP formation results from conformational changes in the enzyme and change in ATP-binding affinity following energization.

Further experiments concerning the voltage dependence of the reversed V-type ATPase, as well as of the activation energy, will help to generate a more complete reaction scheme of the pump process under various physiological conditions.

Acknowledgements. This work was funded by grants from the Deutsche Forschungsgemeinschaft to R. H. and from Consiglio Nazionale delle Ricerche, Italy, and the Herrmann- and Lilly-Schilling-Stiftung to H.A.K. Special project RAISA, subproject N.2.1, paper N. 1142 to F. G. and R. H.

References

Bezanilla F (1985) A high capacity data recording device based on a digital audioprocessor and a video cassetta recorder. Biophys J 47:437–441

Coyaud L, Kurkdjian A, Kado R, Hedrich R (1987) Ion channels and ATP-driven pumps involved in ion transport across the tonoplast of sugar beet vacuoles. Biochim Biophys Acta 902:263–268

Forgac M (1989) Structure and function of vacuolar class of ATP-driven proton pumps. Physiol Rev 69:765–796

Hansen UP, Gradmann D, Sanders D, Slayman CL (1981) Interpretation of current-voltage relationships for "active" ion transport systems: I. Steady-state reaction-kinetic analysis of class-I mechanisms. J Membr Biol 83:165–190

Hedrich R, Kurkdjian A (1988) Characterization of an anion-permeable channel from sugar beet vacuoles: effect of inhibitors. EMBO J 7:3661–3666

Hedrich R, Neher E (1987) Cytoplasmatic calcium regulates voltage-dependent ion channels in plant vacuoles. Nature 329:833–835

Hedrich R, Schroeder JI (1989) The physiology of ion channels and pumps in higher plant cells. Annu Rev Plant Physiol 40:248–268

Hedrich R, Flügge UI, Fernandez JM (1986) Patch-clamp studies of ion transport in isolated plant vacuoles. FEBS Lett 204:228–232

Hedrich R, Kurkdjian A, Guern J, Flügge UI (1989) Comparative studies on the electrical properties of the H^+ translocating ATPase and pyrophosphatase of the vacuolar-lysosomal compartment. EMBO J 8:2835–2841

Läuger P (1991) Electrogenic ion pumps. Vol 5. Sinauer, Sunderland, MA, USA

Lohse G, Hedrich R (1992) Characterization of the plasma membrane H^+-ATPase from Vicia faba guard cells – Modulation by extracellular factors and seasonal changes. Planta 188:206–214

Overath P, Träuble H (1973) Phase transitions in cells, membranes, and lipid of Escherichia coli. Detection by fluorescent probes, light scattering, and dilatometry. Biochemistry 12:2625–2634

Overath P, Gulik-Krzywicky P, Schechter E, Letellier L (1975) Lipid phase transition in cytoplasmic and outer membrane of Escherichia coli. Biochem Biophys Acta 389:358–369

Schneider DL (1987) The proton pump ATPase of lysosomes and related organelles of the vascular apparatus. Biochem Biophys Acta 895:1–10

Senior AR (1988) ATP synthesis by oxidative phosphorylation. Physiol Rev 68:177–2331

Sze H, Ward JM, Lai S (1992) Vacuolar proton-translocating ATPases from plant structure function and isoforms. J Bioenerg Biomembr 24:371–381